3rd International Conference on Advanced Engineering Technologies

19-21 September 2019

Analytical Solution of Continuous Contact Problem in Functionally Graded Layer Resting on Rigid Plane

Yusuf KAYA[*1], Alper POLAT[2], Talat Şükrü ÖZŞAHİN[3]

[1]*Gumuhane University, Civil Engineering Department, Gumushane Turkey*
[2]*MunzurUniversity, Civil Engineering Department, Tunceli, Turkey*
[3]*Karadeniz Technical University, Civil Engineering Department, Trabzon, Turkey*

Keywords:
Continuous contact;
Elasticy;
Functionally graded layer;
Rigid plane;

Abstract

In this study, continuous contact problem for two layers, having different heights and elastic constants, loaded by means of two rigid rectangle stamps and resting on a rigid plane is considered according to theory of elasticity. The problem is solved under the assumptions that all surfaces are frictionless. Using boundary conditions of the problem and integral transform technique, the problem is reduced to a singular integral equation. The integral equation is solved numerically by making use of appropriate Gauss Chebyshev integration formula for rectangular stamp profiles and contact stress distribution under the stamps is obtained. Depending on the contact stress under the stamps, initial separation loads and initial separation distances between the layers and between homogeneous layer and rigid plane are determined.

1 INTRODUCTION

Due to the fact that many structural and mechanical system elements are in contact with each other, contact problems have been widely found in engineering structures. In the cases where the elementary theory is insufficient in the solution of stress, displacement and deformation problems in engineering structures, problems are solved with the help of elasticity theory. In addition, with the development of computer technology and numerical solution methods, the number of studies on this subject has increased significantly. In the literature, various contact problems of the layers are frequently encountered. A number of researchers have discussed contact problems such as continuous and discontinuous contact problem [1-9], contact and crack problem [10-12], frictional and moving contact problem [13-15] and the receding contact problem [16-19] until today.
In this study, the problem of frictionless and continuous contact in a Functionally graded (FG) layer loaded with two rigid flat blocks resting on the homogeneous layer was solved finite analytically. In the problem, the homogeneous layer resting on the rigid plane. The continuous contact problem was solved for different block widths and different height ratios. When the homogeneous layer height is too large, the problem becomes a contact problem in the layer on the elastic half plane. Therefore, the solution was made by increasing the height of the homogeneous layer and the results were compared with [1]. As a result of the solutions, stress distributions under the block, normal stress distributions, initial separation loads and distances were determined.

2 MATERIAL AND METHOD

2.1. Definition of the problem

In this study, the frictionless contact problem of a FG layer resting on a homogeneous layer is solved analytically by using elasticity theory and integral transformation techniques. The FG layer is loaded by rigid two different blocks. The homogeneous layer is resting on a rigid plane. All surfaces are considered to be frictionless and the gravity forces are considered while making the solution. In addition, the rigid blocks are in contact with the FG layer at intervals of (a, b) and (c, d). The layers and the rigid plane extend along the x-axis in the range of $(-\infty, +\infty)$ and the thickness in the z-axis direction is taken as unit.

*e-mail: yusufkaya_29@hotmail.com

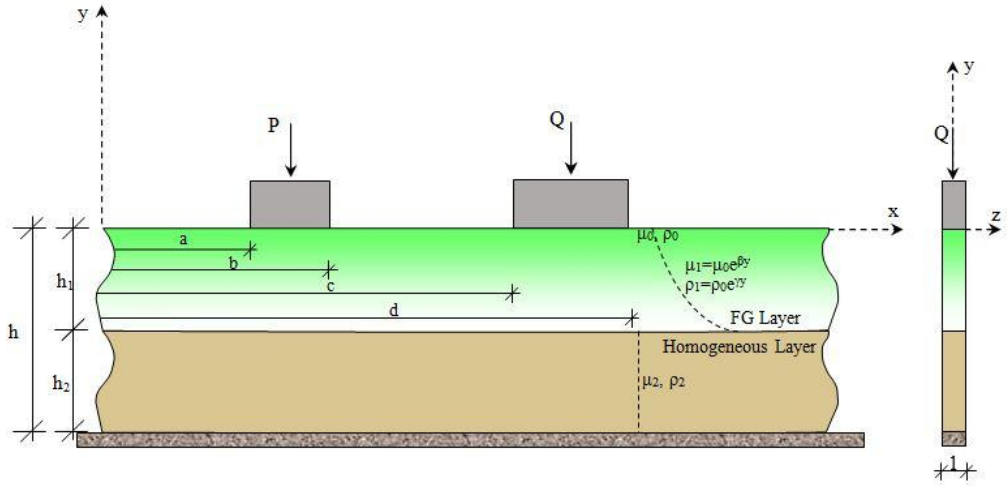

Figure 1. Geometry of the problem

2.2. Analytical Solution of Continuous Contact Problem

First of all, solving the problem, Navier equations were obtained with the help of equilibrium equations, constitutive relation, displacement and strain equations. A set of ordinary differential equations was obtained by applying Fourier integral transformation technique to Navier equations. By solving this set of differential equations, expressions of stresses and displacements were found in terms of unknown coefficients. These unknown coefficients were determined by unknown boundary stresses p (x) and q (x) by the following boundary conditions.

$u(x,y)$ and $v(x,y)$ are displacement components, $\sigma_x(x,y)$, $\sigma_y(x,y)$ and $\tau_{xy}(x,y)$ are stress components and the boundary conditions of the problem can be written as follows according to the axis set in Figure 1:

$$\sigma_{y_1}(x,0)=\begin{cases}-p(x) & a<x<b\\ -q(x) & c<x<d\\ 0 & other\end{cases} \quad (1a)$$

$$\tau_{xy_1}(x,0)=0 \qquad -\infty<x<\infty \quad (1b)$$

$$\tau_{xy_1}(x,-h_1)=0 \qquad -\infty<x<\infty \quad (1c)$$

$$\sigma_{y_1}(x,-h_1)=\sigma_{y_2}(x,-h_1) \qquad -\infty<x<\infty \quad (1d)$$

$$\frac{\partial}{\partial x}\left[v_2(x,-h_1)-v_1(x,-h_1)\right]=0 \qquad -\infty<x<\infty \quad (1e)$$

$$\tau_{xy_2}(x,-h_1)=0 \qquad -\infty<x<\infty \quad (1f)$$

$$\tau_{xy_2}(x,-h)=0 \qquad -\infty<x<\infty \quad (1g)$$

$$v_2(x,-h)=0 \qquad -\infty<x<\infty \quad (1h)$$

$$\frac{\partial}{\partial x}\left[v_1(x,0)\right]=0 \qquad a<x<b \quad (1i)$$

$$\frac{\partial}{\partial x}\left[v_1(x,0)\right]=0 \qquad c<x<d \quad (1j)$$

$p(x)$ and $q(x)$ in equation (1a) are the unknown contact stresses between the rigid block and the functional graded layer.

The equilibrium conditions for the problem are;

$$\int_a^b p(t)\,dt = P \tag{2a}$$

$$\int_c^d q(t)\,dt = Q \tag{2b}$$

After obtaining unknown coefficients, using (1i) and (1j), the singular integral equations can be obtained for $P(x)$ and $Q(x)$ after some simple operations as follow [20]:

$$\begin{aligned} &-\frac{1}{\pi}\frac{1}{\mu_0}\int_a^b p(t_1)dt_1\left[k_1^*(x_1,t_1)+\left(\frac{\kappa_1+1}{4}\right)\frac{1}{(t_1-x_1)}\right] \\ &-\frac{1}{\pi}\frac{1}{\mu_0}\int_c^d q(t_2)dt_2\left[k_1^*(x_1,t_2)+\left(\frac{\kappa_1+1}{4}\right)\frac{1}{(t_2-x_1)}\right]=0 \quad a<x<b \end{aligned} \tag{3a}$$

$$\begin{aligned} &-\frac{1}{\pi}\frac{1}{\mu_0}\int_a^b p(t_1)dt_1\left[k_1^*(x_2,t_1)+\left(\frac{\kappa_1+1}{4}\right)\frac{1}{(t_1-x_2)}\right] \\ &-\frac{1}{\pi}\frac{1}{\mu_0}\int_c^d q(t_2)dt_2\left[k_1^*(x_2,t_2)+\left(\frac{\kappa_1+1}{4}\right)\frac{1}{(t_2-x_2)}\right]=0 \quad c<x<d \end{aligned} \tag{3b}$$

The k_1 kernel in equations is defined as follows;

$$k_1(x,t) = \xi\left(A_1n_1 + A_2n_2 + A_3n_3 + A_4n_4\right) \tag{4}$$

$$k_1^*(x,t) = \int_0^\infty \left(k_1(x,t) - \left(\frac{\kappa_1+1}{4}\right)\sin\xi(t-x)\right)d\xi \tag{5}$$

In order to calculate the contact stresses p(x) and q(x), the equilibrium equations (2) and the integral equations (3) must be solved together.

In the above equations, the material constants of the elastic layers μ_i and κ_i are known as $\kappa_i = (3\text{-}4\upsilon i)$ in the plane deformation and $\kappa_i = (3\text{-}\upsilon_i)/(1 + \upsilon_i)$ in the plane strain. υ_i is Poisson's ratio. For the numerical solution of the integral equation, the following non-dimensional quantities are defined.

To simplify the numerical solution of the integral equation, the following dimensionless quantities are defined:

$$x_1 = \frac{b-a}{2}r_1 + \frac{b+a}{2} \qquad t_1 = \frac{b-a}{2}s_1 + \frac{b+a}{2} \tag{6a-b}$$

$$x_2 = \frac{d-c}{2}r_2 + \frac{d+c}{2} \qquad t_2 = \frac{d-c}{2}s_2 + \frac{d+c}{2} \tag{6c-d}$$

$$g_1(s_1) = \frac{p\left(\frac{b-a}{2}s_1 + \frac{b+a}{2}\right)}{P/h_1} \qquad g_2(s_2) = \frac{q\left(\frac{b-a}{2}s_1 + \frac{b+a}{2}\right)}{P/h_1} \tag{6e-f}$$

λ refers to the load factor. In the case where the load factor (λ) gets up to a certain critical value (λ_{cr}), it becomes a separation between the layers or between the homogeneous layer and the rigid plane and the

problem becomes a discontinuous contact problem. The distance that the initial separation occurs is called the initial separation distance (x_{cr}).
Here g(s) are dimensionless contact stresses that occur on rigid blocks. Since the contact stresses at the sides of the rigid blocks have singularity, the index of the integral equation is +1. Accordingly, the solution of the singular integral equation is sought as follows:

$$g_i(s_i) = G_i(s_i)\left[1-s_i^{\,2}\right]^{-1/2} \qquad (-1 < s_i < 1) \qquad (i = 1,2) \tag{7}$$

Here, g (s) is limited to a closed range of -1 ≤ s ≤ 1. Using the appropriate Gauss-Chebyshev integration formula, the equations (2) and (3) can be reduced to the following state.

$$-\sum_{i=1}^{n} W_i G_1(s_{1i}) \frac{b-a}{2h}\left[m_1(r_1,s_1) + \left(\frac{\kappa_1+1}{4}\right) \frac{1}{\frac{b-a}{2}(s_{1i}-r_{1j})} \right]$$

$$-\sum_{i=1}^{n} W_i G_2(s_{2i}) \frac{d-c}{2h}\left[m_2(r_1,s_2) + \left(\frac{\kappa_1+1}{4}\right) \frac{1}{\left[\frac{d-c}{2}s_{2i}+\frac{d+c}{2}\right]-\left[\frac{b-a}{2}r_{1j}+\frac{b+a}{2}\right]} \right] = 0$$

$$(j = 1,\ldots,n-1) \tag{8}$$

$$-\sum_{i=1}^{n} W_i G_1(s_{1i}) \frac{b-a}{2h}\left[m_3(r_2,s_1) + \left(\frac{\kappa_1+1}{4}\right) \frac{1}{\left[\frac{b-a}{2}s_{1i}+\frac{b+a}{2}\right]-\left[\frac{d-c}{2}r_{2j}+\frac{d+c}{2}\right]} \right]$$

$$-\sum_{i=1}^{n} W_i G_2(s_{2i}) \frac{d-c}{2h}\left[m_4(r_2,s_2) + \left(\frac{\kappa_1+1}{4}\right) \frac{1}{\frac{d-c}{2}(s_{2i}-r_{2j})} \right] \qquad (j = 1,\ldots,n-1) \tag{9}$$

The terms in these equations are defined as follows;

$$W_1 = W_n = \frac{1}{2n-2} \qquad W_i = \frac{1}{n-1} \qquad (i = 2,\ldots,n-1) \tag{10}$$

$$s_{1i} = s_{2i} = \cos\left(\frac{i-1}{n-1}\pi\right) \qquad (i = 1,\ldots,n) \qquad \text{(a)}$$

$$r_{1i} = r_{2i} = \cos\left(\frac{2j-1}{2n-2}\pi\right) \qquad (j = 1,\ldots,n-1) \qquad \text{(b)} \tag{11 a-b}$$

After the stresses σy_1 (x, -h_1) and σy_2 (x, -h) on the contact surfaces have been determined by adding the gravity forces and performing the necessary intermediate operations, the expressions giving the initial separation loads and the initial separation distances are obtained as follows:

$$\sigma_{1y}(x,y) = 2P\frac{e^{\beta y}}{(\kappa_1-1)}\int_0^{\infty}\sum_{j=1}^{4}\left[i\xi(3-\kappa_1)+s_j n_j(\kappa_1+1)\right]A_j e^{s_j y}\left[\cos\xi(t-x)\right]d\xi +$$

$$2Q\frac{e^{\beta y}}{(\kappa_1-1)}\int_0^{\infty}\sum_{j=1}^{4}\left[i\xi(3-\kappa_1)+s_j n_j(\kappa_1+1)\right]A_j e^{s_j y}\left[\cos\xi(t-x)\right]d\xi + \frac{\rho_0 g(e^{\gamma y}-1)}{\gamma} \qquad 0 < x < \infty \tag{12}$$

$$\sigma_{y_2}(x,y) = 2P\mu_2\int_0^{\infty}\left\{ e^{-|\xi|y}\left\{-2|\xi|B_1+\left[(\kappa_2-1)-2|\xi|y\right]B_2\right\} + e^{|\xi|y}\left\{2|\xi|B_3+\left[(\kappa_2-1)+2|\xi|y\right]B_4\right\}\right\}\left[\cos\xi(t-x)\right]d\xi +$$

$$2Q\mu_2\int_0^\infty\left\{e^{-|\xi|y}\left\{-2|\xi|B_1+\left[(\kappa_2-1)-2|\xi|y\right]B_2\right\}+e^{|\xi|y}\left\{2|\xi|B_3+\left[(\kappa_2-1)+2|\xi|y\right]B_4\right\}\right\}\left[\cos\xi(t-x)\right]d\xi+$$

$$\frac{\rho_0 g(e^{-\gamma h_1}-1)}{\gamma}+\rho_0 gy \quad 0<x<\infty \tag{13}$$

For the FG layer, the load factor formula becomes to following, in the case of the load get up to the critical load $(P=P_{cr})$;

$$\lambda_{cr_1}=\frac{P_{cr}}{\rho_0 g{h_1}^2} \tag{14a}$$

The critical load factor formula that cause initial separation in the homogeneous layer is obtained as follow

$$\lambda_{cr_2}=\frac{P_{cr}}{\rho_0 g{h_1}^2+\rho_2 g{h_2}^2} \tag{14b}$$

3 RESULTS

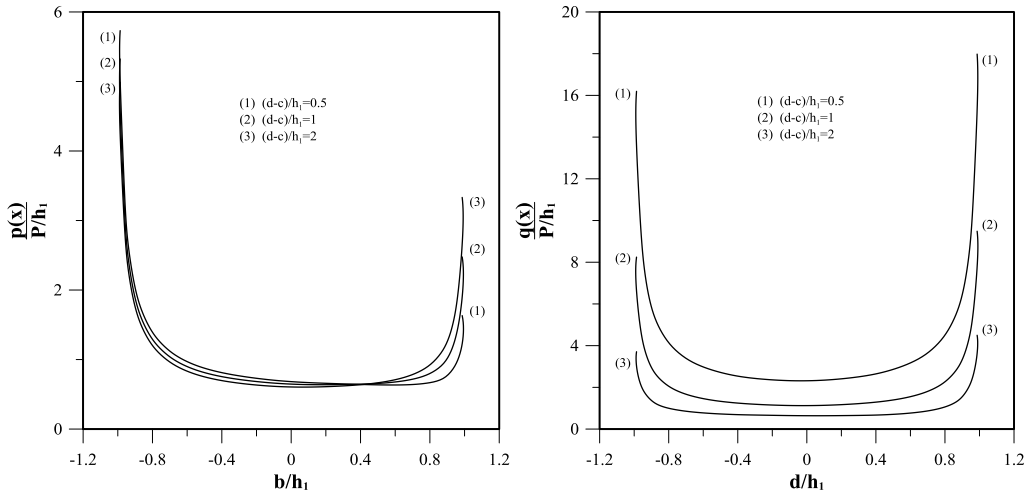

Figure 2 (a-b). Distribution of contact stresses under block for various block width values (a/h_1=3, $(b-a)/h_1$=1, $(c-b)/h_1$=1, βh_1=0.6931, γh_1=0.6931, Q/P=2, κ_1=1, κ_2=1, μ_2/μ_{-h1}=1, h_1/h=0.5)

Figure 2 shows the dimensionless contact stress distribution under the block for various block widths. As can be seen from the figure, as the block width increases, the stresses decrease under the block will as the force will spread over a larger area.

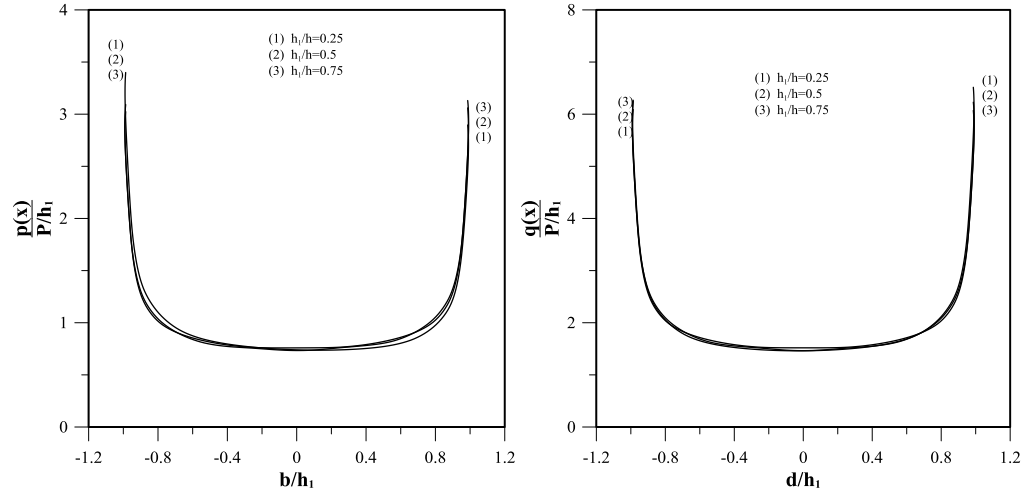

Figure 3 (a-b) Distribution of contact stresses under block for various h_1/h values (a/h_1=3, $(b-a)/h_1$=1, $(c-b)/h_1$=2, $(d-c)/h_1$=1, βh_1=-1.3862, γh_1=-1.0986, Q/P=2, κ_1=1, κ_2=1, μ_2/μ_{-h1}=1)

Figure 3 shows the dimensionless contact stress distribution under the block for various ratios h_1/h. As can be seen from the figure, the change in the layer height ratios does not cause very big changes under the block. The increase in the h_1/h ratio creates a slight increase under the block.

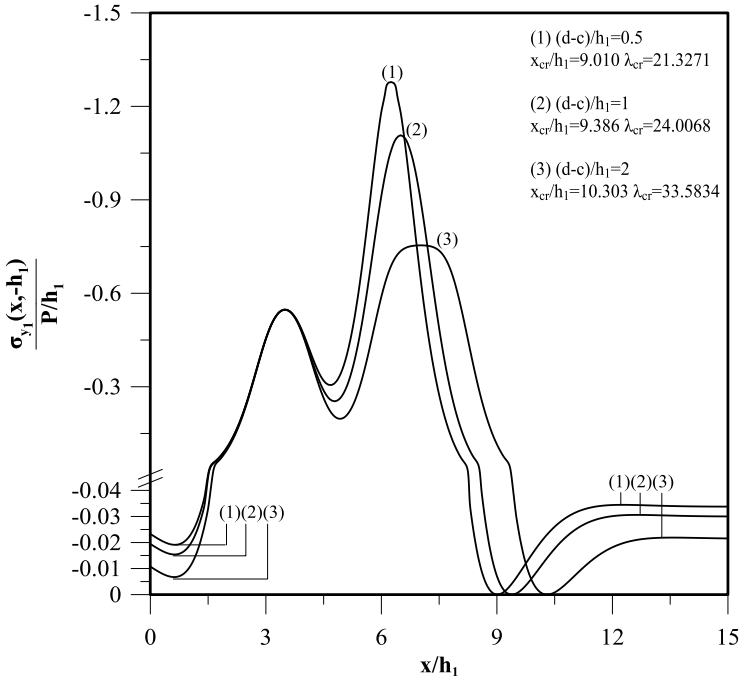

Figure 4a. Distribution of σ_y stresses between layers for various block width values (a/h_1=3, $(b-a)/h_1$=1, $(c-b)/h_1$=1, βh_1=0.6931, γh_1=0.6931, Q/P=2, κ_1=1, κ_2=1, μ_2/μ_{-h1}=1, h_1/h=0.5)

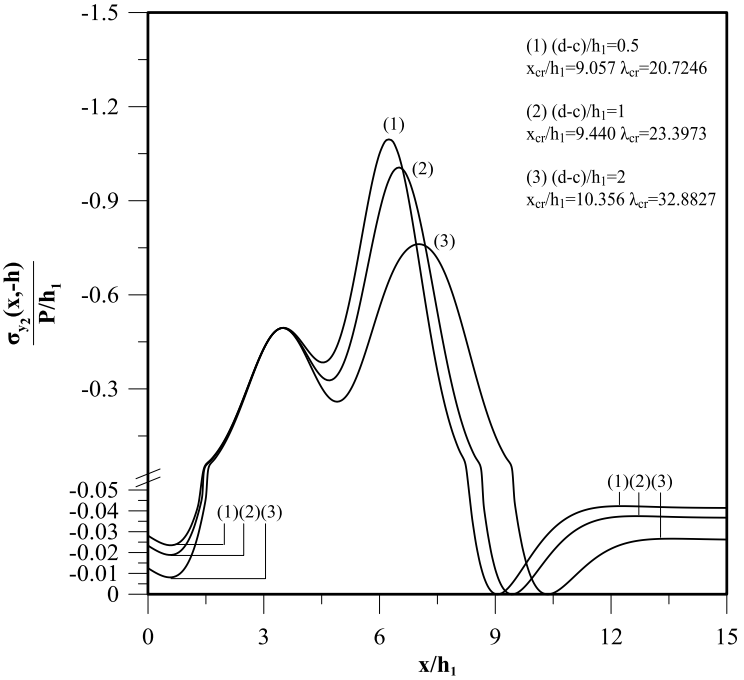

Figure 4b. Distribution of σ_y stresses between the homogeneous layer and the rigid plane for various block width values (a/h_1=3, $(b-a)/h_1$=1, $(c-b)/h_1$=1, βh_1=0.6931, γh_1=0.6931, Q/P=2, κ_1=1, κ_2=1, μ_2/μ_{-h1}=1, h_1/h=0.5)

In Figure 4 a, b, dimensionless σy_1 $(x,-h_1)/(P/h_1)$ and σy_2 $(x,-h)/(P/h_1)$ contact stress distributions according to various $(d-c)/h_1$ values are given respectively. For this loading case where the load of the second block is taken 2 times higher, it is seen that the stresses decrease when the ratio $(d-c)/h_1$ increases, that is, if the width of the second block increases. In addition, when Figure 4 is examined, the point where the initial separation occurs is increased as the block width increases and the initial separation load increases.

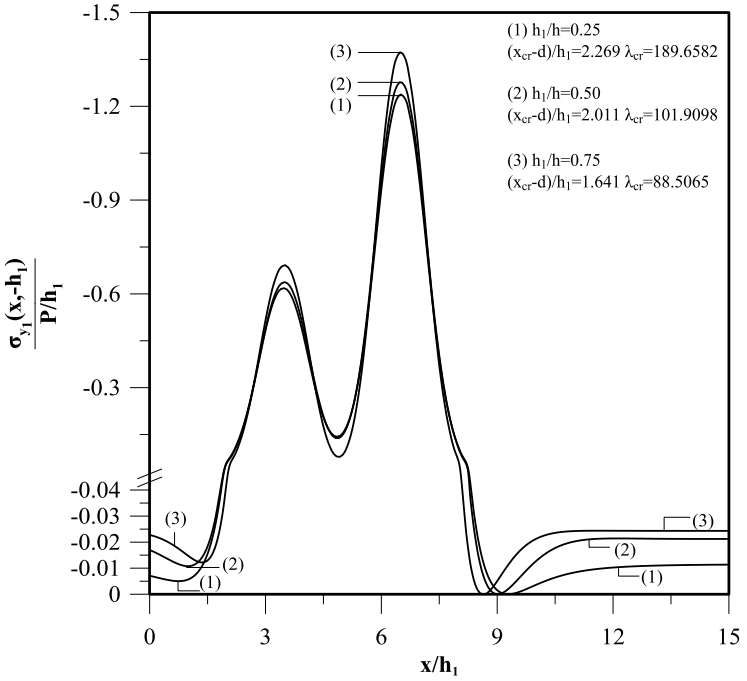

Figure 5a. Distribution of contact stresses between FG layer and homogeneous layer for various h_1/h values (a/h_1=3, $(b-a)/h_1$=1, $(c-b)/h_1$=2, $(d-c)/h_1$=1, βh_1=-1.0986, γh_1=-1.3862, Q/P=2, κ_1=1, κ_2=1, μ_2/μ_{-h1}=1)

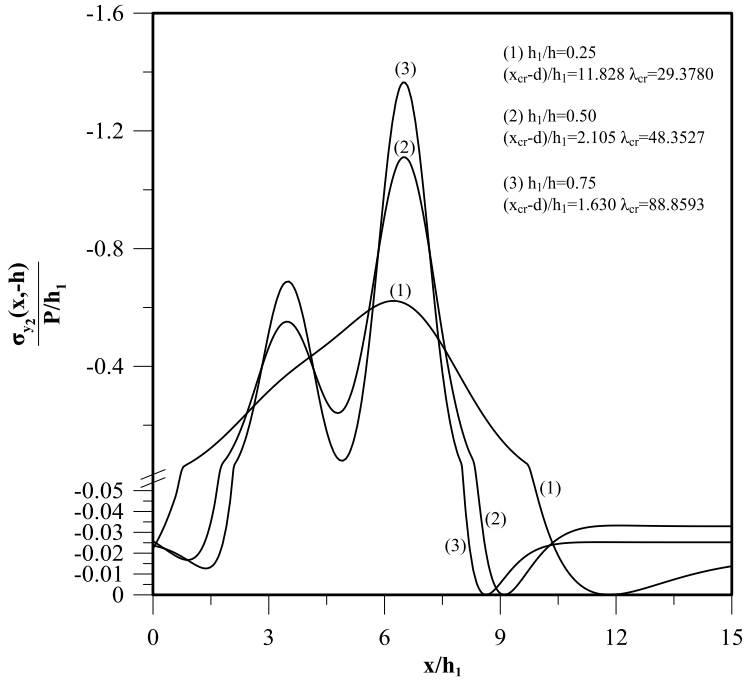

Figure 5b. Distribution of contact stresses between the homogeneous layer and the rigid plane for various h1/h values (a/h_1=3, $(b-a)/h_1$=1, $(c-b)/h_1$=2, $(d-c)/h_1$=1, βh_1=-1.0986, γh_1=-1.3862, Q/P=2, κ_1=1, κ_2=1, μ_2/μ_{-h1}=1)

In Figure 5 a,b, the contact stress distributions without dimension $\sigma y_1(x,-h_1)/(P/h_1)$ and $\sigma y_2(x,-h)/(P/h_1)$, respectively, according to various h_1/h values are given. In this loading where the load of the second block is taken 2 times more, it is seen that the stresses increase in the case of the increase of the h_1/h ratio, the decrease of the height of the second layer. Further, when Fig. 5 is examined, the point at which the initial separation occurs as the h_1/h ratio increases, but as this ratio increases, the initial separation load for the second layer decreases while the initial separation load for the second layer increases.

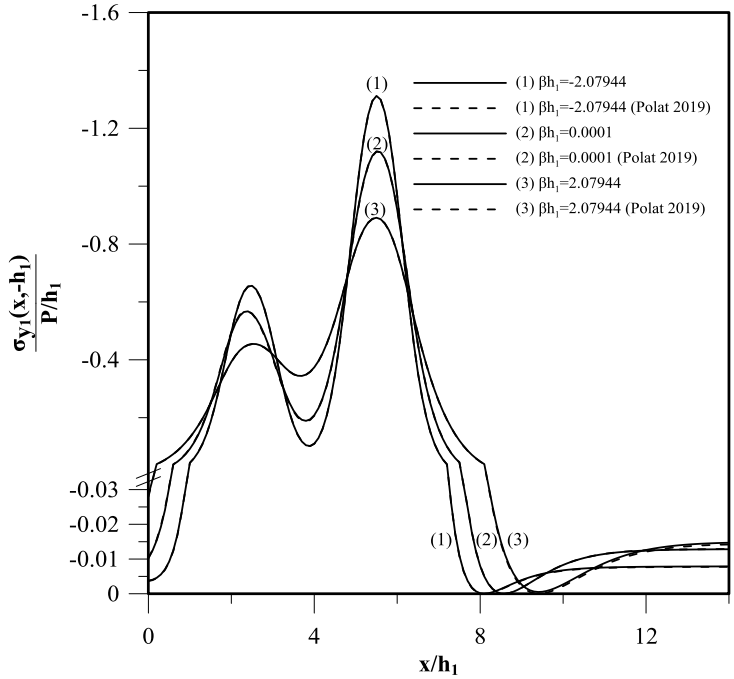

Figure 6. The dimensionless $\sigma y_1(x,-h_1)/(P/h_1)$ contact stress distribution between the FG layer and the elastic semi-infinite plane for various βh_1 values ($a/h_1=2$, $(b-a)/h_1=1$, $(c-b)/h_1=2$, $(d-c)/h_1=1$, $\mu_0=1$, $\mu_2/\mu_{-h1}=1$, $\gamma h_1=-0.6931$, $y=-h_1$, $h_1=1$, $h_1/h=0.1$ $\kappa_1=\kappa_2=2$, $Q=2P$)

Table 1. Variation of the initial separation load and distances between the layers for various βh_1 values when the height of the homogeneous layer increases ($a/h_1=2$, $(b-a)/h_1=1$, $(c-b)/h_1=2$, $(d-c)/h_1=1$, $\mu_0=1$, $\mu_2/\mu_{-h1}=1$, $\gamma h_1=-0.6931$, $y=-h_1$, $h_1=1$, $h_1/h=0.1$ $\kappa_1=\kappa_2=2$, $Q=2P$)

βh_1	x_{cr}/h_1		Error	λ_{cr}		Error
	This Study	Polat (2019)	(%)	This Study	Polat (2019)	(%)
-2.07944	8.12	8.13	0.12	181.724	181.958	0.128
0.0001	8.58	8.58	0.00	110.998	110.784	0.193
2.07944	9.44	9.41	0.31	99.302	99.011	0.294

If the height of the homogeneous layer increases, the problem is similar to the contact problem in the layer that fits the elastic half plane. Therefore, by increasing the height of the second layer, the problem was compared with [Polat 2018]. In Figure 6, dimensionless $\sigma_{y1}(x,-h_1)/(P/h_1)$contact stress distribution according to various βh_1 values is given. In Figure 6 and Table 1, in this loading case where the second block load is taken 2 times more, when the upper surface stiffness of the layer is higher than the lower surface, in other words, as the βh1 stiffness parameter value increases, the separation occurs at the farther point, while the initial separation loads decrease. If the stiffness of the lower surface of the layer is higher than the top, the separation load increases, while the layer is separated from the plane closer to the blocks. As shown in Figure 6 and Table 1, the results are highly consistent each other.

4 CONCLUSION

- When the block width $(d-c)/h_1$ increases, the stresses decrease under the block. Because, the force will spread over a larger area.
- Change in the layer height ratios (h_1/h) does not cause very big changes under the block. The increase in the h_1/h ratio creates a slight increase under the block.
- The σy_1 and σy_2 stresses decrease when the ratio $(d-c)/h_1$ increases, that is, if the width of the second block increases.
- When the block width increases, initial separation distance and the initial separation load increases.
- The σy_1 and σy_2 stresses increase in the case of the increase of the h_1/h ratio, as the decrease of the height of the second layer.

- The point at which the initial separation occurs as the h_1/h ratio increases, but as this ratio increases, the initial separation load for the second layer decreases while the initial separation load for the second layer increases.
- When the upper surface stiffness of the layer is higher than the lower surface, in other words, as the βh_1 stiffness parameter value increases, the separation occurs at the farther point, while the initial separation loads decrease. If the stiffness of the lower surface of the layer is higher than the top, the separation load increases, while the layer is separated from the plane closer to the blocks.
- When this study compared to [1] it seen that this solution and ref. [1] are very closed each other.

References

[1] Polat, A., Kaya, Y., Özşahin, T.Ş. (2018). Analytical solution to continuous contact problem for a functionally graded layer loaded through two dissimilar rigid punches. Meccanica, 53(14), 3565-3577.

[2] Kaya, Y., Polat, A., Özşahin T.Ş.: Comparıson of FEM Solution with Analytical Solution of Continuous and Discontinuous Contact Problem, Sigma Journal of Engineering and Natural Sciences, 36, 4, pp:977-992 (2018).

[3] A. Polat, Y. Kaya, T.Ş. Özşahin, (2018)," Frictionless Contact Problem for a Functionally Graded Layer Loaded Through Two Rigid Punches Using Finite Element Method, Journal of Mechanics, DOI: 10.1017/jmech.2018.55.

[4] T.Ş. Özşahin. V. Kahya, A. O. Çakıroğlu. "Contact Problem for an Elastic Layered Composite Resting on Rigid Flat Supports", *International Journal of Computational and Mathematical Sciences*, 1, 2, 145-159, 2007.

[5] Adiyaman G., Öner E., Birinci A., 2017. Continuous and discontinuous contact problem of a functionally graded layer resting on a rigid foundation, Acta Mechanica, vol.0, pp.1-10.

[6] Çakıroğlu, F. L., Çakıroğlu, M. ve Erdöl, R., 2001. Contact Problems for Two Elastic Layers Resting on Elastic Half-Plane, Journal of Engineering Mechanics, 127, 2, 113-118.

[7] Kahya, V., 2003. İki Tabakalı Elastik Ortamda Sürekli ve Süreksiz Temas Problemlerinin İncelenmesi, Doktora Tezi, K.T.Ü, Fen Bilimleri Enstitüsü, Trabzon.

[8] Özşahin, T.Ş., 2000. Rijit İki Blok Üzerine Oturan Bileşik Tabakada Sürekli ve Süreksiz Temas Problemi, Doktora Tezi, KTÜ Fen Bilimleri Enstitüsü, Trabzon.

[9] Y. Kaya, A. Polat, T.Ş. Özşahin. Analysis Of Continuous Contact Problem Of Homogeneous Plate Bonded A Rigid Support By Using Finite Element Method, 2nd International Conference On Advanced Engineering Technologies (Icadet 2017), 21-23 September 2017 Bayburt, Turkey.

[10] Ben-Romdhane, M., El-Borgi, S. ve Charfeddine, M., 2013; An Embedded Crack in a Functionally Graded Orthotropic Coating Bonded to a Homogeneous Substrate Under a Frictional Hertzian Contact. International Journal of Solids and Structures, 50, 3898–3910.

[11] Adıbelli, H., 2010. Elastik Yarım Düzleme Oturan Simetrik Yüklü Yapışık Çift Tabakada Değme ve Çatlak Problemi, Yüksek Lisans Tezi, Fen Bilimleri Enstitüsü, KTÜ.

[12] Rekik M., Neifar M., El-Borgi S., 2010. An Axisymmetric Problem of an Embedded Crack in a Graded Layer Bonded to a Homogeneous Half-Space, International Journal of Solids and Structures, 47, 2043–2055.

[13] Guler, M.A., Kucuksucu, A., Yılmaz, K.B., Yıldırım, B. (2017). On the analytical and finite element solution of plane contact problem of a rigid cylindrical punch sliding over a functionally graded orthotropic medium. Int J Mech Sci 120:12–29.

[14] Talezadehlari A., Nikbakht A., Sadighi M. Ve Zucchelli A., 2016. Numerical Analysis of Frictional Contact in The Presence of a Surface Crack in a Functionally Graded Coating Substrate System, International Journal of Mechanical Science, 117, 286-298.

[15] Su, J., Ke L.L., El- Borgi, S., Xiang, Y. ve Wang Y.S., 2018. An effective method for the sliding frictional contact of conducting cylindirical punch on FGPMs, International Journal of Solids and Structures, 141-142, 127-136.

[16] Yan J. ve Mi C., 2017. On the Receding Contact between an Inhomogeneously Coated Elastic Layer and a Homogeneous Half-Plane, Mechanics of Materials, 112, 18-27.

[17] Yılmaz, K. B., Çömez, İ., Yıldırım, B., Güler, M. A. ve El-Borgi, S., 2018. Frictional Receding Contact Problem for a Graded Bilayer System Indented by a Rigid Punch, International Journal of Mechanical Sciences, 141, 127–142.

[18] El-Borgi, S., Çömez, İ., 2017. A Receding Frictional Contact Problem Between a Graded Layer and a Homogeneous Substrate Pressed by a Rigid Punch, Mechanics of Materials, 114, 201–214.

[19] Adiyaman G., Birinci A., 2018. A general solution for the receding contact problem of a functionally graded layer resting on a Winkler foundation. Journal of Structural Engineering & Applied Mechanics, vol.1 (3) pp. 136-146.

[20] Erdogan, F., Gupta, G.: On the numerical solutions of singular integral equations, Quart. J. Appl. Math. vol. 29, pp. 525-534 (1972)